Proceedings of the 3rd International Congress APMAS2013, April 24–28, 2013, Antalya, Turkey

Structural Analysis of Ce Doped $La_{1-x}Sr_xCo_{1-y}Fe_yO_{3-\delta}$ Nanopowders Synthesized by Glycine-Nitrate Gel Combustion

Ö. Yildiz[a,*], A.M. Soydan[b], A. Ata[b], E.F. İpçizade[b], D. Akin[b] and Ö. Uçak[b]

[a]Kocaeli University, Faculty of Engineering, Department of Metallurgical and Materials Engineering TR-41380 Kocaeli, Turkey

[b]Gebze Institute of Technology, Faculty of Engineering, Department of Materials Science and Engineering TR-41400 Gebze/Kocaeli, Turkey

Ce doped $La_{1-x}Sr_xCo_{1-y}Fe_yO_3$ (LCSCF) is a widely used cathode material due to its high catalytic activity for oxygen reduction and high oxygen exchange coefficient. LCSCF is also known with its high ionic and electronic conductivities and low electrode polarization losses which are highly critical properties for low temperature solid oxide fuel cell applications. In this study, structural properties of the LCSCF cathode nanopowder materials synthesized by glycine–nitrate gel combustion have been investigated by X-ray diffraction, differential scanning calorimetry, scanning electron microscopy, and nanosizer. Synthesized nanopowders represent volcanic ash like structures and morphologies. Ce, Sr, Co, and Fe are found to have significant effects on the structural properties of powders in terms of powders morphology, agglomerate structure, crystallite size and also lattice parameter of perovskite crystal. All synthesized ash powders have particle sizes around 50–600 nm, varying crystalline structures of perovskite and fluorite depending on molar ratio of Ce in the composition. Increasing molar Ce ratio over 0.4 is found to lead to the formation of a separate nano ceria phase in fluorite crystal structure on the surface of the synthesized powder.

DOI: 10.12693/APhysPolA.125.669

PACS: 81.07.Wx, 81.07.−b, 81.20.Ka, 88.30.pn

1. Introduction

Solid oxide fuel cells (SOFCs) which convert chemical energy into electrical energy have been drawing attention due to their high efficiency and fuel flexibility [1, 2]. However, they need to be improved in terms of their performance and mechanical properties. The structural properties of the materials used have significant effects on overall performances and mechanical properties. One of the sluggish mechanisms taking place on SOFCs is the oxygen reduction reaction that takes place on the cathode layer. Several research groups have been focusing on a novel cathode material with high conductivity and mechanical durability.

Reducing the operating temperature from 1000 °C down to intermediate (600–800 °C) and low (< 600 °C) temperature ranges was an important goal for many researchers [2, 3]. Lower operating temperatures increase the ohmic resistance and polarization losses [4, 5]. On the other hand, ohmic and polarization losses can be minimized with thinner electrodes [4], active catalytic materials [5], optimized electrode microstructures [6], or combination of ionically and electronically conductive materials [5]. It is a well known fact that cathode polarization loss is the most important potential of low temperature SOFCs. Novel materials are required to decrease the polarization losses at the cathode layer and ionic resistance at cathode–electrolyte interface.

LSCF's are considered as good cathode materials due to their ionic and electronic conductivity at low and intermediate temperatures [7]. They also have high catalytic activity for oxygen reduction reaction due to their good oxygen surface exchange and self-diffusion properties [6]. Ionic and electronic conductivities as well as oxygen reduction reaction activities are much higher for sub-oxidized LSCFs ($La_{1-x}Sr_xCo_{1-y}Fe_yO_{3-\delta}$) [4, 8]. However, the self-diffusion of oxygen through the LSCFs necessitates the use of an interlayer between the cathode and the electrode [1, 4, 9]. Gadolinium doped ceria (GDC) can be used to prevent oxygen diffusion [1, 4, 9].

Several cathode materials and dopant alternatives have been evaluated for high fuel cell performance [4, 6, 7, 10–12]. Firstly, Ce doped LSCF was investigated. Enhanced ionic conductivity and electrocatalytic activity were observed while coarsening was prevented [6, 10]. Secondly, the effect of $Sr_{1-a}Ce_aFe_{1-b}Co_bO_{3-x}$ (SCFC) cathode material on fuel cell performance was studied with different Ce and Co contents by Trofimenko and Ullmann [4]. Fuel cell performance was found to be increasing with increasing Co content and decreasing Ce content [4]. Furthermore, the performance of GDC-impregnated LSCF was found to be dependent on the nano-GDC phase [11]. Triple phase boundary (electrolyte–porosity–cathode) points were more commonly obtained with nanosized GDC materials with high surface areas [7, 11–13]. In another study, cathode infiltration with Samarium doped Ceria (SDC) nanoparticles on LSCF was applied. Lower polarization loss was obtained in comparison with blank LSCF [11–14]. Finally, the strong effect of powder morphology and chemical composition on fuel cell performance has been reported in previous literature [7, 11–14].

In this study, Ce doped $La_{1-x}Sr_xCo_{1-y}Fe_yO_{3-\delta}$ nanopowders were synthesized by glycine–nitrate gel combustion (GNGC) as cathode materials for low temperature SOFCs. Structural analyses of the synthe-

*corresponding author; e-mail: oyildiz@kocaeli.edu.tr

sized powders were performed with analytical methods. GNGC process was chosen to synthesize nanopowders due to its simplicity, cost effectiveness, high productivity and ability to synthesize homogeneous structure with desired structural properties like particle and crystallite size, morphology and agglomerate structure.

2. Experimental

La(III)-nitrate $\{La(NO)_3{\cdot}6H_2O\}$, Ce(III)-nitrate $\{Ce(NO)_3{\cdot}6H_2O\}$, Sr-nitrate $\{Sr(NO_3)_2\}$, Co-nitrate $\{Co(NO_3)_2{\cdot}6H_2O\}$, and glycine ($NH_2CH_2CO_2H$) from Alfa Aesar with a purity of 99.0% were used as starting raw materials.

2.1. Synthesis of LCSCF nanopowders

Cathode nanopowders with changing compositions synthesized by GNGC are given in Table. Calculated metal–nitrate compositions and glycine–nitrate mixture were dissolved at pure water. Heat was applied to the solution throughout mixing. With increasing temperature and time, the solution became a highly viscous jelly structure which was safely located into a custom combustion reactor for the formation of the nanopowders. The combustion reaction took place at around $\approx 230\,^{\circ}C$ (Fig. 1).

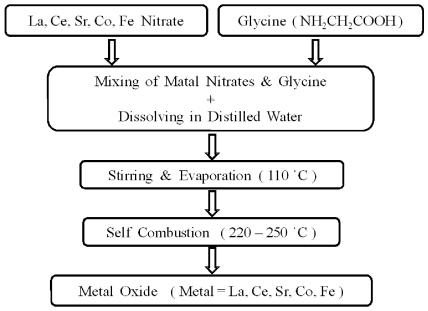

Fig. 1. Glycine nitrate gel combustion steps for synthesis of nanopowders.

TABLE

Synthesized nanopowder compositions of the cathode materials.

No.	Composition
1	$(La_{0.6}Ce_{0.0}Sr_{0.4})(Co_{0.8}Fe_{0.2})O_3$
2	$(La_{0.6}Ce_{0.2}Sr_{0.2})(Co_{0.8}Fe_{0.2})O_3$
3	$(La_{0.6}Ce_{0.4}Sr_{0.0})(Co_{0.8}Fe_{0.2})O_3$
4	$(La_{0.4}Ce_{0.4}Sr_{0.2})(Co_{0.8}Fe_{0.2})O_3$
5	$(La_{0.2}Ce_{0.6}Sr_{0.2})(Co_{0.8}Fe_{0.2})O_3$
6	$(La_{0.2}Ce_{0.6}Sr_{0.2})(Co_{0.7}Fe_{0.3})O_3$
7	$(La_{0.2}Ce_{0.6}Sr_{0.2})(Co_{0.6}Fe_{0.4})O_3$
8	$(La_{0.3}Ce_{0.5}Sr_{0.2})(Co_{0.5}Fe_{0.5})O_3$
9	$(La_{0.2}Ce_{0.5}Sr_{0.3})(Co_{0.5}Fe_{0.5})O_3$
10	$(La_{0.2}Ce_{0.4}Sr_{0.4})(Co_{0.4}Fe_{0.6})O_3$
11	$(La_{0.2}Ce_{0.4}Sr_{0.4})(Co_{0.3}Fe_{0.7})O_3$
12	$(La_{0.2}Ce_{0.4}Sr_{0.4})(Co_{0.2}Fe_{0.8})O_3$

2.2. Characterization of LCSCF nanopowders

The crystallinity and crystal structure of the synthesized powders were investigated by X-ray diffraction (XRD) Rigaku Dmax2200 Diffractometer and Cu K_α radiation with the wavelength of 1.54060 Å was used in XRD analysis. Thermal behaviors of the powders were observed by differential scanning calorimeter (DSC) with STA 449C from Netzsch. The microstructural characterization such as particle size, shape and morphology were performed by scanning electron microscopy (SEM) type XL30 SFEG from Philips. The particle size and size distribution were measured by ZS-Nanosizer 2000 from Malvern Instruments.

3. Results and discussion

In this study, structural properties of the Ce doped $La_{1-x}Sr_xCo_{1-y}Fe_yO_{3-\delta}$ nanopowders for low temperature SOFC cathode materials were investigated. Powders are found to represent varying morphological and structural properties depending on the type and molar ratio of the dopant materials (Ce, Sr, Fe, and Co). Synthesized powders generally exhibit volcanic-tuff-like shapes and morphologies [15], and nanoscale particle sizes as shown in Figs. 2 and 3. Liu and Zhang [13] reported the fabrication of nanostructured and functionally graded composite cathodes, which are graded in microstructure as well as in composition, using a combustion CVD process. Their results indicated that nanostructured electrodes significantly reduce the interfacial polarization of cathode/electrolyte. Analyzing the SEM images with 20000× and higher magnifications of crude powder samples, it is observed that all the powders produced are nanosized. As an illustration, 20000× magnification SEM images of samples 5 and 7 presented in Fig. 2 clearly show that the powders are nanosized. Synthesized crude powders still preserve their nanosize characteristics after being exposed to heat treatment freely at 900 °C during one hour treatment, with no use of any pressing process (Fig. 3, sample 4).

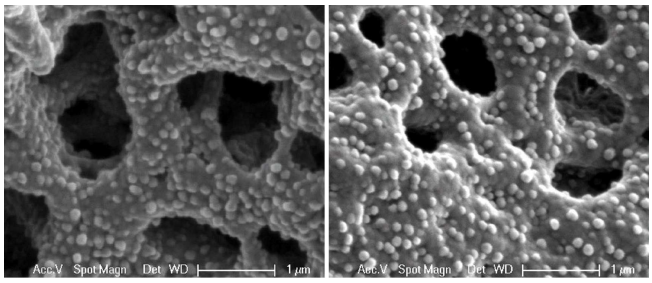

Fig. 2. SEM images of nanopowders synthesized by glycine nitrate gel combustion (samples 5 and 7).

In the case of having higher Sr, La, and Co composition, the produced crude powders are in thin structured, big porous, volcanic ash-like morphologies (Fig. 4, samples 1, 2, and 3). When forming a big porous structure, Sr, La, and Co have significant roles [16, 17]. In the event of high Ce and Co concentrations, powders with thin structured small porous morphologies are formed [16] (Fig. 4, samples 3, 4, 5 and 6). It has been observed

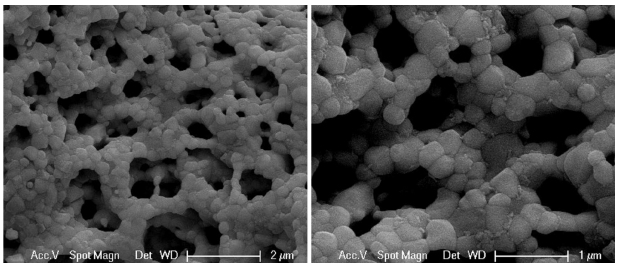

Fig. 3. SEM images of synthesized nanopowders (sample 4) heated at 900 °C for 1 h.

that with the increment of Ce concentration, crystallite size decreases [16, 18, 19] (Fig. 5). Leng and Chan [18] concluded that increasing the content of Ce in LSCF, LSCF–Ce cathode showed more homogeneous pore structure and distribution, smaller particle size, and less particle agglomeration. Besides, the decrement of Sr and La leads to small-sized pores and agglomerate structured powders (Fig. 4, samples 4, 5, and 6). When considering the SEM images at Fig. 4, the compositions in Table, and crystallite sizes in Fig. 5 together, a specific relation between pores, agglomerate structure, and crystallite size with component composition [17] is clearly seen. While the powders with high concentrations of Sr, La and Co have big porous, thin structured morphologies (Fig. 4, samples 1, 2 and 3), the powders with high concentration of Fe still display big porous (depends on La and Sr concentration), but more condense and massive structures (Fig. 4, samples 10, 11, and 12). With the increment in Ce, Fe and the decrement in La, Sr concentrations correspondingly, powders are inclined to have smaller sized agglomerate structures (Fig. 4, samples 4, 5, and 6). On the other hand, nanoparticle formation rate in agglomerate surfaces increases with Ce concentration (Figs. 2 and 3, samples 5, 6, and 7). However, depending on the increment of Fe concentration, a dense and massive structure occurs and these nanoparticles on the surface disappear in the main structure (Fig. 4, samples 10, 11, and 12).

XRD analysis of the samples revealed single perovskite phase product [17]. All of the synthesized ash powders have crystalline structures as shown in Fig. 6. It was determined that the powders which do not have Ce in their contents have crystalline structures as shown in Fig. 6. While the proportion of Sr decreases and Ce increases in the compositions of high Co, ceria based powders having fluorite crystalline structure are formed (Fig. 6, samples 3, 4, 5, and 6) as shown in the SEM images (Fig. 2 and Fig. 4, samples 5, 6, and 7). However, although the Ce proportion is as high as 0.4 mole, fluorite crystalline structure could not be observed due to the fact that Fe ratio is higher than 0.7 mole (Fig. 6, samples 11 and 12). Powders with merely perovskite crystal structure are formed. Along with the alteration of component compositions, the other most effective factors are the ionic radii and the value of the valence of each cation has while forming the crystallite structure. In the case of

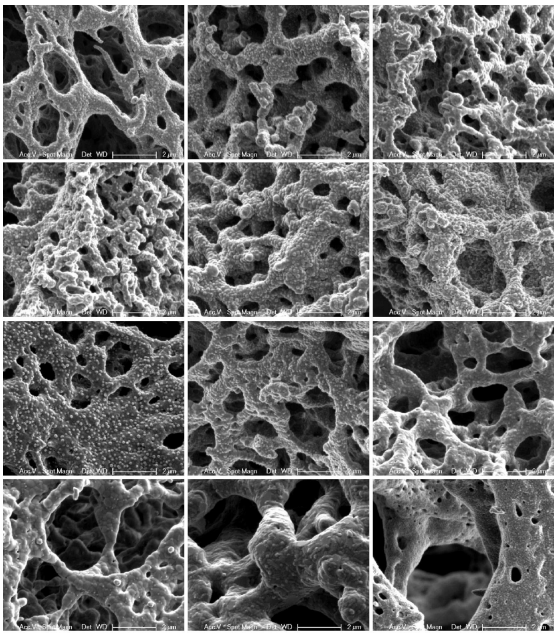

Fig. 4. SEM images of all nanopowders synthesized by glycine nitrate gel combustion (samples 1,2,3//4,5,6//7,8,9//10,11,12).

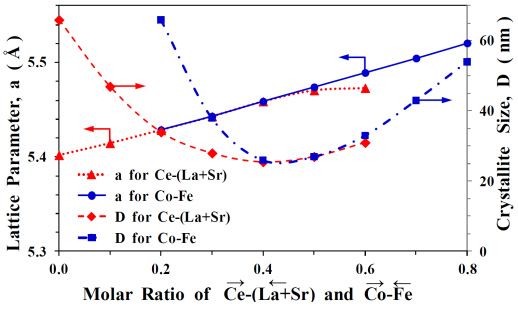

Fig. 5. Lattice parameter (a) of perovskite crystal structure and crystallite size (D) of the synthesized nanopowders calculated from XRD analysis results.

high proportions of La and Sr, Co atoms may be located in the center of the perovskite crystal structure. However, depending on the decrement of Sr and increment of Ce, the lattice parameter increases. The lattice parameter decreases with decreasing La proportion (Fig. 5) and because of the inconsistency, the powder is formed to some extent with a fluorite crystal structure (Fig. 6, samples 3, 4, 5 and 6). In the case of decrease of the Co proportion and increase of the Fe proportion, it is just possible to produce powders that have only perovskite crystal structure (Fig. 6, samples 11 and 12).

Figure 5 shows the lattice parameter of the crystal structure and the crystallite sizes of synthesized ash nanopowders which are determined from the XRD analysis results. Lattice parameter decreases with increases of Ce in La–Ce proportions as well as with increases of Sr in Ce–Sr proportions. On the other hand, the lattice parameter decreases while decreasing Co and increasing Fe.

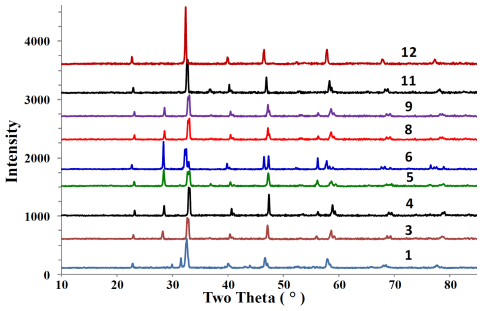

Fig. 6. XRD analysis of nanopowders synthesized by glycine nitrate gel combustion.

It is determined that Ce, Co and Fe are the most important components to affect the crystallite size (Fig. 5). As the ratio of Ce and Co increases, the size of the crystallite is reduced. Furthermore, when the ratio of Fe increases, the size of crystallite swells and forms more massive agglomerate structures. Although it is clearly seen that the powders which have been produced are nanosized, bigger values have been obtained according to the results of XRD and SEM images at high magnifications (Fig. 7). The most essential point that draws attention is the agglomeration of powders that have large surface areas due to balance of surface electric and the difficulty of dispersement. Hence, the difficulties have been encountered in the SEM, TEM, and nanosizer characterization of nanopowders.

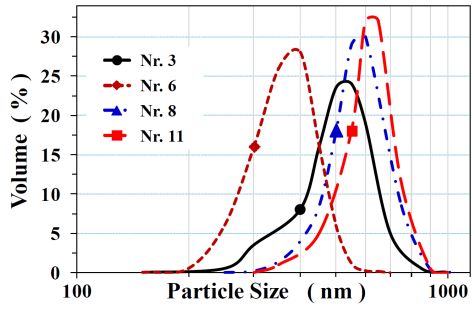

Fig. 7. Particle size analysis of nanopowders (samples 3, 6, 8, and 11) synthesized by glycine nitrate gel combustion.

On the evaluation of properties of nanopowders that have been produced, it is clearly seen that the compositions within numbers 4 and 9 have quite outstanding features as Ce doped $La_{1-x}Sr_xCo_{1-y}Fe_yO_{3-\delta}$ cathode material. LSCF cathode materials with ceria nanoparticles on the grain surface have low polarization resistances [3–5]. Also, the powder morphology and chemical composition of the starting materials have important influences on the decrease of cathodic polarization resistance as well as increase of the fuel cell performance [1]. As a consequence, the mole fractions of cathodes in the compositions that used Ce doped $La_{1-x}Sr_xCo_{1-y}Fe_yO_{3-\delta}$ cathodes have to be in that range; $0.4 \leq Ce \leq 0.6$, $0.2 \leq La \leq 0.4$, $Sr \leq 0.3$, $0.4 \leq Co < 0.6$ and $0.4 \leq Fe \leq 0.6$. On the other hand, the electrical properties of the cathode materials which will be produced from such composition ranges at various working conditions must be investigated.

4. Conclusions

Ce doped $La_{1-x}Sr_xCo_{1-y}Fe_yO_{3-\delta}$ nanopowders as cathode materials for low and intermediate temperature SOFCs can be synthesized in desired powder characteristics by GNGC. The properties of the nanopowders such as agglomerate structure, morphology, particle size and distribution, and crystallite size can be optimized by changing the cathode material compositions. Powders obtained by using cations with large ionic radii between $0.4 \leq Ce \leq 0.6$, $0.2 \leq La \leq 0.4$, $Sr \leq 0.3$ ratios and small ionic radii in $0.4 \leq Co < 0.6$ and $0.4 \leq Fe < 0.6$ ratios have been observed to result in the most suitable powder characteristics for LSCF cathode powder manufacturing.

Acknowledgments

This work was supported by Turkish Ministry of Science, Industry and Technology and Kale Group under the contract San-Tez 00892.STZ.2011-1.

References

[1] S.M. Haile, *Acta Mater.* **51**, 5981 (2003).
[2] S.C. Singhal, *Solid State Ion.* **135**, 305 (2000).
[3] S.P. Jiang, W. Wang, *Solid State Ion.* **176**, 1351 (2005).
[4] N.E. Trofimenko, H. Ullmann, *J. Europ. Ceram. Soc.* **20**, 1241 (2000).
[5] H.Y. Tu, Y. Takeda, N. Imanishi, O. Yamamoto, *Solid State Ion.* **100**, 283 (1997).
[6] C. Sun, R. Hui, J. Roller, *J. Solid State Electrochem.* **14**, 1125 (2010).
[7] J.H. Kim, H. Kim, *Ceram. Int.* **38**, 4669 (2012).
[8] J.H. Kim, Y.M. Park, H. Kim, *J. Power Sources* **196**, 3544 (2011).
[9] V. Dusastre, J.A. Kilner, *Solid State Ion.* **126**, 163 (1999).
[10] N.A. Baharuddin, H.A. Rahman, A. Muchtar, A.B. Sulong, H. Abdullah, *J. Zhejiang University-Science A (Appl. Phys. Eng.)* **14**, 11 (2013).
[11] L. Nie, M. Liu, Y. Zhang, M. Liu, *J. Power Sources* **195**, 4704 (2010).
[12] W. Kim, H. Song, J. Moon, H. Lee, *Solid State Ion.* **177**, 3211 (2006).
[13] B. Liu, Y. Zhang, *J. Alloys Comp.* **453**, 418 (2008).
[14] C.P. Kashinath, S.T. Aruna, T. Mimani, *Curr. Opinion Solid State Mater. Sci.* **6**, 507 (2002).
[15] Ö. Yıldız, A.M. Soydan, A. Ata, B. Tunaboylu, D. Akin, E.F. Ipcizade, *Acta Phys. Pol. A* **123**, 432 (2013).
[16] D. Bouchard, L. Sun, F. Gitzhofer, G.M. Brisard, *J. Thermal Spray Technol.* **15**, 37 (2006).
[17] T. Striker, J.S. Ruud, Y. Gao, W.J. Heward, C. Steinbruchel, *Solid State Ion.* **178**, 1326 (2007).
[18] Y. Leng, S.H. Chan, *Int. J. Hydrogen Energy* **33**, 3808 (2008).
[19] Z. Shao, W. Zhou, Z. Zhu, *Prog. Mater. Sci.* **57**, 804 (2012).